

## **ELECTROMAGNETIC SCATTERING OF THE FIELD OF A METAMATERIAL SLAB ANTENNA BY AN ARBITRARILY POSITIONED CLUSTER OF METALLIC CYLINDERS**

**C. A. Valagiannopoulos**

Department of Radio Science and Engineering  
School of Electrical Engineering, Aalto University  
5A Otakaari St., Espoo, FIN-02150, Finland

**Abstract**—The operation of a slab antenna with low-index metamaterial substrate is affected by a cluster of metallic cylinders positioned in the near-field area. A semi-analytical solution of the defined boundary value problem is obtained based on the small size of the rods. Several different configurations are found to possess beneficial features concerning the total radiated power and the angle of directive emission. The deduced diagrams are independently validated and discussed, revealing certain conclusions.

### **1. INTRODUCTORY COMMENTS**

Slab configurations with radiating and propagating properties have been extensively investigated in numerous publications. It has been stated [1] that a metamaterial ground plane can exhibit certain incidence angle-dependent reflection phases in order to support directional emissions. Similar structures can be utilized in designing a bianisotropic cloak fixed in a uniformly moving medium, according to the findings presented in [2]. The coordinate transformation technique has been also employed in examining Cartesian metamaterial substrates which not only improve the directive emission but also enhance the radiation efficiency as the dipole feed gets closer and closer to the metallic reflector [3]. Furthermore, transition slab layers have

---

*Received 30 December 2010, Accepted 16 February 2011, Scheduled 18 February 2011*  
Corresponding author: Constantinos A. Valagiannopoulos (konstantinos.valagiannopoulos@aalto.fi).

been used for matching a structure of a backward-wave transmission-line network, with free space, performing a tuning procedure of the network impedance [4].

On the other hand, multiple metallic rods are commonly utilized in electromagnetic devices in order to acquire desirable characteristics. It has been shown [5] that an array of metamaterial cylinders increases forward scattering cross section, which may contribute in reinforcing the directivity of antennas. In another interesting work [6], the use of tiny metallic cylinders is proposed to discretize the perimeter of perfectly conducting scatterers providing reliable solutions to scattering problems. Additionally, an effective procedure has been developed for the analysis of the electromagnetic interaction with metallic polygonal cylinders based on the analytical regularization of the integral equations [7].

In this work, we combine the two aforementioned concepts (slab antennas, multiple cylinders) by considering a cluster of metallic pins which scatters the produced field of a centrally-fed metamaterial slab antenna. Similar radiating backgrounds have been extensively analyzed in many other works [8–15], while metamaterial geometries are considered in numerous treatises and studies [16–21]. Investigations on planar structures are contained in several analyses [22–28] and scattering is broadly examined in works such as [29] and [30]. Semi analytical solutions are of prime importance in research regardless of the scientific domain they are referred to. These approximate approaches are the key factors to produce simple models imitating the function of far more complicated systems. Given the fact that commercial numerical techniques are usually hiding the physical mechanisms and the traditional purely analytical methods cover only few unrealistic configurations, semi analytical solutions are meaningful in most cases. That is why we followed that path in the present report. The set of conducting cylinders positioned into the near field of the antenna could have a modulating role which can adjust some features of the radiator at will. In other words, it can be used as tool correcting or regulating the characteristics of the original device. By exploiting the electrically small size of the scatterers, simple formulas are obtained whose reliability is validated through simulation software. Several different cluster configurations are analyzed; for each of them, the power gain and the maximum power direction are represented as functions of the operational frequency and the geometrical parameters of the problem. The produced diagrams are discussed and certain applicable conclusions are drawn from them.

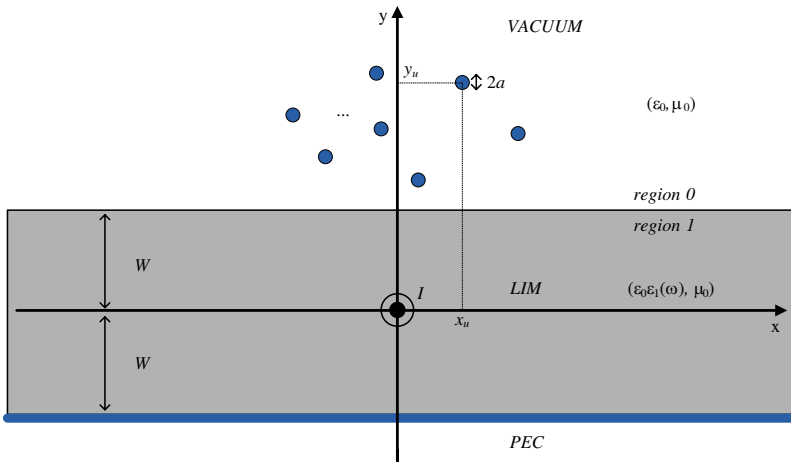


Figure 1. The configuration of the analyzed structure.

## 2. SOLUTION DERIVATION

### 2.1. Problem Statement

The physical configuration of the examined device is shown in Fig. 1, where the considered Cartesian coordinate system  $(x, y, z)$  is also defined. An infinite dipole of current  $I$  (in *Amperes*) is located centrally into a slab of finite thickness  $2W$  (region 1), filled with a low-index metamaterial (LIM) of relative permittivity  $\epsilon_1(\omega)$ . This dielectric volume is backed by a reflecting metallic screen posed at  $y = -W$ , while the whole structure is located into vacuum (region 0). This specific type of antenna is preferred because it has been found to possess substantial directivity properties. It is also a state-of-the-art structure which can be extensively used in the future and thus it is worth to examine the effect of the additional equipment on this device. There are several textbooks analyzing the configuration, the excitation and the characteristics of the low-index metamaterial slab antenna. For example in [31] the radiating properties of this structure are presented and discussed. The developed field is scattered by a cluster of  $U$  identical perfectly conducting (PEC) cylinders of small radius  $a \ll W$ , placed at arbitrary positions  $(x, y) = (x_u, y_u)$ ,  $u = 1, \dots, U$ , parallel to  $z$  axis. Low index metamaterials are plasmonic substances working close to their resonant frequency  $\omega_P$ . In particular, a simplified form of  $\epsilon_1(\omega)$  is given by:

$$\epsilon_1(\omega) = \frac{\omega^2 - \omega_P^2}{\omega^2}, \quad (1)$$

where  $\omega$  is the operating circular frequency of a harmonically dependent time  $e^{+j\omega t}$ . The resonant frequency of a plasmonic substance can be estimated through various techniques. Numerous studies have been performed in measuring the plasma frequency of dielectric materials as chromium [32] or superconducting ones like in Levitated Dipole Experiment [33]. Moreover it is rather common to assume the parameter of the host substances as well-known [34]. All the areas are magnetically inert, while, due to the symmetry, the electric field of each region is  $z$ -polarized. In the following analysis, the symbols  $k_0 = \omega\sqrt{\epsilon_0\mu_0}$ ,  $k_1 = k_0\sqrt{\epsilon_1(\omega)}$  are used for the operating wavenumbers in free-space and LIM slab respectively. In addition, the well-known radiation functions defined by:  $g_{0/1}(\beta) = \sqrt{\beta^2 - k_{0/1}^2}$ , are always evaluated with a nonnegative real part (and in case it zero, with a positive imaginary part).

The scope of this work is to provide a semi-analytical treatment to the defined boundary value problem which is in accordance with results derived from commercial software simulations. Also, we aim at estimating the beneficial or disadvantageous effect of this random pin lattice on the propagation features and the radiation characteristics of the considered device. The novelty of the presented structure does not lie in the sort of the radiator which is well-known, but in the scattering cluster of pins which is located within the near field. The positive or the damaging influence of a set of electrically small cylinders on the operation of this antenna has not yet investigated neither analytically nor numerically.

## 2.2. Absent Cluster

Let us reproduce the explicit formulas of some quantities referring to the structure in the absence of this grid of thin cylindrical scatterers. The Green's function of electric type, in our example, equals the axial electric field when the structure is excited by a filamentary electric current with magnitude  $\frac{j}{\omega\mu_0}$  (in *Amperes*). When the infinite dipole is located along the axis  $(x, y) = (X, Y)$ , the Green's function for any obstacle to the vacuum region 0 ( $Y > W$ ), is comprised by the singular free-space term describing the effect of the dipole itself, added to the smooth term expressing the influence of the slab antenna. The singular term is defined as follows:

$$\begin{aligned} G_n(x, y, X, Y) &= -\frac{j}{4}H_0^{(2)}\left(k_0\sqrt{(x-X)^2 + (y-Y)^2}\right) \\ &= \frac{1}{4\pi}\int_{-\infty}^{+\infty}\frac{e^{-g_0(\beta)|y-Y|}}{g_0(\beta)}e^{-j\beta(x-X)}d\beta. \end{aligned} \quad (2)$$

The notation  $H_0^{(2)}$  corresponds to the 0th-order Hankel function of second type. The smooth component is given by:

$$G_m(x, y, X, Y) = \int_{-\infty}^{+\infty} C_G(\beta) e^{-j\beta(x-X) - g_0(\beta)(y+Y)} d\beta, \quad (3)$$

where the integrand function  $C_G(\beta)$  has been rigorously determined:

$$C_G(\beta) = \frac{e^{2Wg_0(\beta)} g_0(\beta) \sinh(2Wg_1(\beta)) - g_1(\beta) \cosh(2Wg_1(\beta))}{4\pi g_0(\beta) g_0(\beta) \sinh(2Wg_1(\beta)) + g_1(\beta) \cosh(2Wg_1(\beta))}. \quad (4)$$

The incident electric field into region 0, where the cluster of pins is positioned, owns the form:

$$E_{0,inc}(x, y) = \int_{-\infty}^{+\infty} C_E(\beta) e^{-j\beta x - g_0(\beta)y} d\beta, \quad (5)$$

where:

$$C_E(\beta) = -\frac{e^{Wg_0(\beta)}}{2\pi} \frac{j\omega\mu_0 I \sinh(Wg_1(\beta))}{g_0(\beta) \sinh(2Wg_1(\beta)) + g_1(\beta) \cosh(2Wg_1(\beta))}. \quad (6)$$

Note that for  $W \rightarrow 0$  the electric field vanishes, which makes sense because the opposite image of the source neutralizes the effect of the excitation dipole. Detailed derivations of the aforementioned formulas are contained in [35].

### 2.3. Present Cluster

It is common knowledge that the basic analytic tool for treating scattering problems is the so-called scattering integral [36]. This pivotal formula, written for the scattered field inside vacuum region 0, is particularized in our case to give:

$$E_{0,scat} = -j\omega\mu_0 \sum_{u=1}^U \oint_{S(u)} \kappa_u [G_n + G_m] dl, \quad (7)$$

where  $S(u)$  is the metallic surface of the  $u$ th PEC pin and  $\kappa_u$  the unknown (supposedly constant) axial,  $z$ -polarized current (in  $A/m$ ) flown upon it. Due to the small radius of the pin, we are going to impose the boundary conditions for vanishing field around the metallic rods, only on  $U$  specific points: the centers of the circular bounds. That yields to:

$$E_{0,inc}(x_v, y_v) + E_{0,scat}(x_v, y_v) = 0, \quad (8)$$

for  $v = 1, \dots, U$ . Let us compute the scattering field at these discrete positions  $(x, y) = (x_v, y_v)$ . Due to the electrically small cross section

of the metallic rods, the smooth integrands in (7), exhibit negligible variation around them and thus, the corresponding line integrals can be approximately evaluated as follows:

$$\oint_{S(u)} \kappa_u G_m(x_v, y_v, X, Y) dl \cong \kappa_u M_{vu} = \kappa_u 2\pi a G_m(x_v, y_v, x_u, y_u). \quad (9)$$

As far as the singular components are concerned, the integrals are analytically evaluated via a standard procedure [37]:

$$\begin{aligned} & \oint_{S(u)} \kappa_u G_n(x_v, y_v, X, Y) dl \cong \kappa_u N_{vu} \\ & = \kappa_u \frac{\pi a}{2j} \begin{cases} H_0^{(2)}(k_0 a) & v = u \\ J_0(k_0 a) H_0^{(2)}\left(k_0 \sqrt{(x_v - x_u)^2 + (y_v - y_u)^2}\right) & v \neq u. \end{cases} \quad (10) \end{aligned}$$

In this sense, a  $U \times U$  linear system with respect to the unknown vector  $\boldsymbol{\kappa} = [\kappa_u]$ , is formulated:

$$[\mathbf{M} + \mathbf{N}] \cdot \boldsymbol{\kappa} = \frac{1}{j\omega\mu_0} \mathbf{e}_{\text{inc}}, \quad (11)$$

where  $\mathbf{M} = [M_{vu}]$  and  $\mathbf{N} = [N_{vu}]$  for  $v, u = 1, \dots, U$ . Obviously, the constant vector contains the samples of the incident field at the centers of the pins, namely:  $\mathbf{e}_{\text{inc}} = [E_{0,\text{inc}}(x_v, y_v)]$ . Once the unknown currents are determined, the scattering field can be approximately computed by (7), namely:

$$E_{0,\text{scat}}(x, y) = -2\pi a j\omega\mu_0 \cdot \sum_{u=1}^U \kappa_u [G_n(x, y, x_u, y_u) + G_m(x, y, x_u, y_u)]. \quad (12)$$

If one introduces the equivalent cylindrical coordinate system  $(\rho, \phi, z)$  and the corresponding notation  $(\rho_u, \phi_u)$ ,  $u = 1, \dots, U$  for the pins axes, the asymptotic relations for the developed field in the far region  $\{\rho \rightarrow +\infty, \phi \in (0, \pi)\}$ , could be derived. Implementation of stationary phase approximation [38] yields to:

$$e_{0,\text{inc}}(\phi) \sim \pi k_0 C_E(k_0 \cos \phi) \sin \phi, \quad (13)$$

$$e_{0,\text{scat}}(\phi) \sim -2\pi a j\omega\mu_0 \cdot$$

$$\sum_{u=1}^U \kappa_u \left[ \pi k_0 C_G(k_0 \cos \phi) e^{jk_0 \rho_u \cos(\phi + \phi_u)} \sin \phi - \frac{j}{4} e^{jk_0 \rho_u \cos(\phi - \phi_u)} \right], \quad (14)$$

for  $\rho \rightarrow +\infty$ . The  $\rho$ -dependent factor  $\sqrt{\frac{2}{\pi k_0 \rho}} e^{-jk_0 \rho + j\frac{\pi}{4}}$  is omitted and that is why the small letter  $e$  is used in defining the field quantities instead of the total ones which are denoted by  $E$ .

### 3. NUMERICAL RESULTS

Prior to proceeding to the numerical simulation and commenting on the produced graphs, the value range of the input parameters should be clarified. The plasma frequency of the low-index metamaterial is kept fixed throughout the examples:  $\omega_P = 20\pi \text{Grad/sec}$  and the operational frequency is selected close to  $\omega_P$ . The thickness of the slab  $2W$  is chosen on the order of a centimeter, while the radius  $a$  of the pins possesses much lower values. As far as the output parameters are concerned, two are the quantities of interest: (I) The direction along which the maximum power is radiated by the antenna, denoted by  $\phi_{\max}$  ( $\phi_{\max} = 90^\circ$  when the lattice of pins is absent); (II) The ratio of the radiated power in the presence of the cylinders over the power emitted without them:

$$R = |e_{0,inc}(\phi) + e_{0,scat}(\phi)|^2 / |e_{0,inc}(\phi)|^2. \quad (15)$$

A set of computer programs has been developed to implement the derived formulas (11), (12) and compute the functions (13), (14) from which the desired quantities  $\phi_{\max}$ ,  $R$ , are determined.

To validate the produced results, we used the Ansoft HFSS commercial simulator for evaluating the electric field within the considered configuration. Even though the boundary conditions on the axes of the metallic rods have been checked, it is sensible to seek an independent way to verify the evaluated quantities. In Fig. 2, the error of the described technique in computing the near electric field ( $y = 2W$ ) is shown as function of the horizontal distance for various pins positioning. It is remarkable that the difference in any case does not surpass 3% which leads to much more accurate results for the far field quantities. In this sense, we are permitted to use the extracted expressions to formulate the following diagrams containing reliable data.

In Fig. 3, we examine the case of  $U$  metallic pins being uniformly distributed along a straight line with inclination angle  $\theta$  (see Fig. 3(a)). The positions of the rods are given by:

$$x_u = a + (4u - 1)a \cos \theta, \quad y_u = W + a + (4u - 1)a \sin \theta, \quad (16)$$

for  $u = 1, \dots, U$ . In Fig. 3(b), we represent the direction of maximum radiated power  $\phi_{\max}$  as function of the slope  $\theta$  for various operating frequencies. It is noted that when the inclination of the distribution line is kept low, the maximum power is radiated close to  $\phi = 90^\circ$  (as does the antenna itself, in the absence of the scatterers). This means that the scattering cluster does not affect significantly  $\phi_{\max}$  when it is posed far from the vertical direction. On the other hand, there is a rapid increase in  $\phi_{\max}$  close to  $\theta \cong 60^\circ$  and then the measured quantity

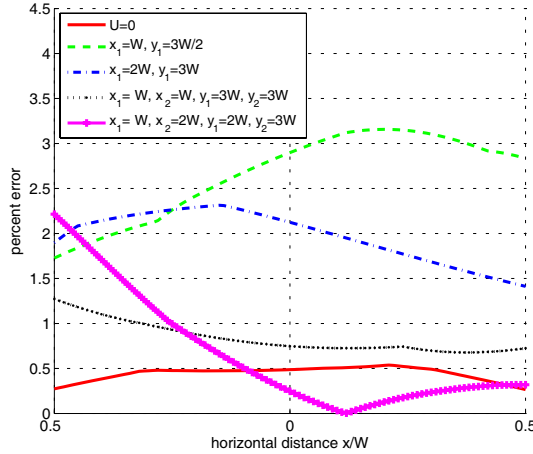


**Figure 2.** The difference between the results obtained through the described semi-analytical technique and those derived via simulation commercial package, as function of the horizontal distance for various pins configurations. Plot parameters:  $\omega_P = 20 \pi \text{Grad}/\text{sec}$ ,  $\omega = 1.5\omega_P$ ,  $a = 0.09 \text{ mm}$ ,  $W = 3 \text{ mm}$ ,  $I = 1 \text{ A}$ .

decreases gradually. This increase is more abrupt for frequencies close to plasma limit  $\omega \cong \omega_P$ , while for a small  $\omega = 0.75\omega_P$ , the curve is relatively smooth.

In Fig. 3(c), the power ratio  $R$  is represented with respect to the oscillation frequency for several  $\theta$ . For small angles, the ratio of the radiated power surpasses unity, regardless of the oscillation frequency. This is attributed to the substantial scattering effect of the pins set, in case it is located close to the maximal directivity angle of the antenna. One can also observe that close to plasma frequency, the ratio is locally maximized in all cases except for  $\theta = 45^\circ$ . Mind also the low-frequency secondary peak recorded in the case of  $\theta = 25^\circ$ . In addition, the curves are oscillating more rapidly, the smaller is the slope angle, which means that, with such a choice of parameters, the signal sensitivity of the device is increased.

In Fig. 4, we consider that the cylinders are located across two, symmetric with respect to the vertical axis, lines as illustrated in Fig. 4(a). The positions are the same as in Fig. (3a) but here we assume two “subclusters” comprised of  $U/2$  scatterers each, forming a “radiation funnel”. In Fig. 4(b), we show the variation of the power ratio  $R$  with respect to operating frequency for various angles  $\theta$ . A very large peak is recorded, just before the resonant frequency, when

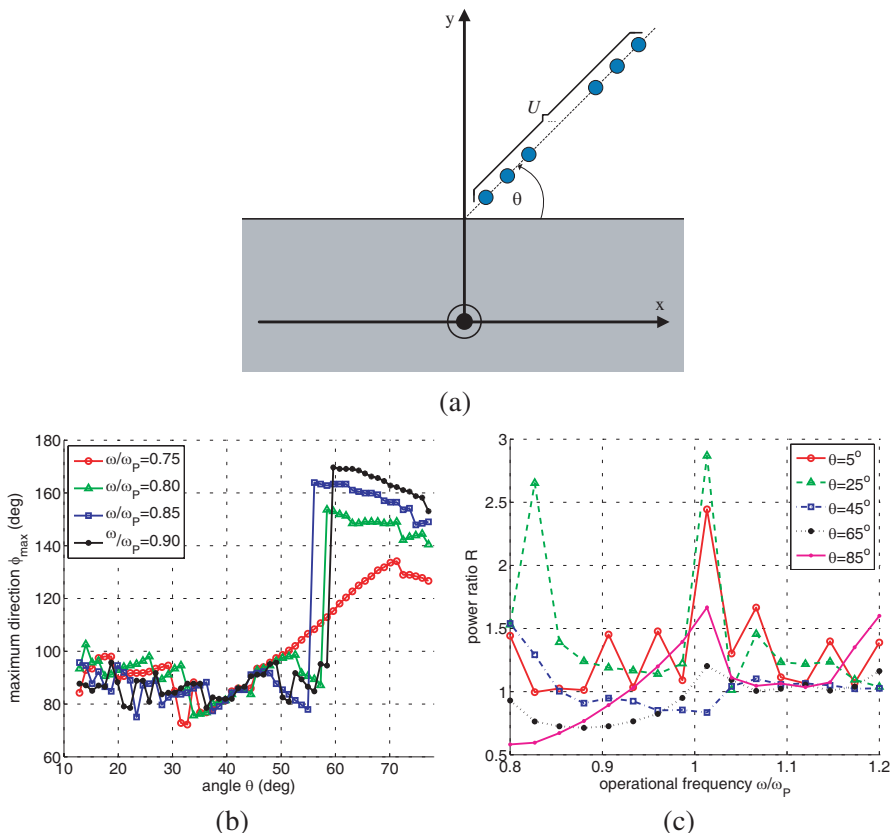
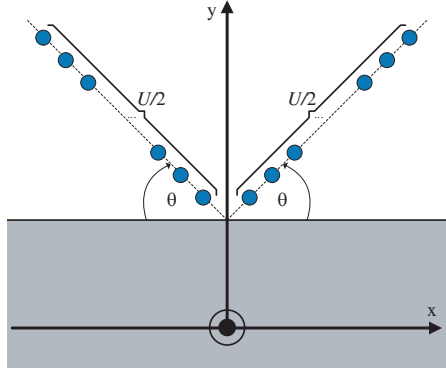
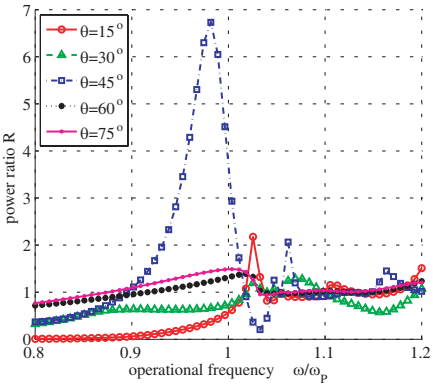


**Figure 3.** (a) The examined case of multiple pins uniformly distributed along a straight sloping line, (b) the maximum power angle as function of the line’s slope for various frequencies, (c) the radiated power ratio as function of the operational frequency for several slopes. Plot parameters:  $\omega_P = 20 \pi \text{Grad}/\text{sec}$ ,  $a = 5 \text{ mm}$ ,  $W = 30 \text{ mm}$ ,  $I = 1 \text{ A}$ ,  $U = 12$ .

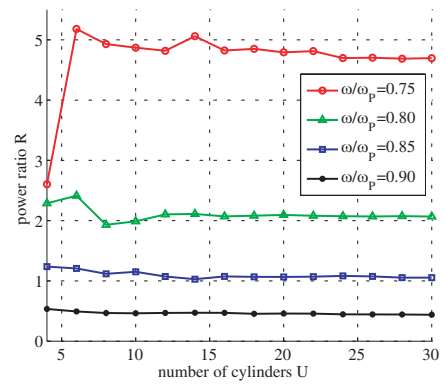
the two lines of the pins are normal each other. With this combination of input quantities, the positioning of the metallic rods reinforces the radiated power. In other words, it diminishes that portion of power being reflected back to the source due to the material discontinuity at  $y = W$ . In this sense, the lattice of pins could play a “matching” role, maximizing the transmitted power from the source to the outer space. When the angular extent is large (small  $\theta$ ), the performance of the device gets poor; in particular, for  $\omega < \omega_P$  the ratio  $R$  is negligible. On the other hand, when  $\omega > \omega_P$ , the measured  $R$  is found close to



(a)



(b)



(c)

**Figure 4.** (a) The examined case of two symmetric grids of cylinders forming a radiation funnel, (b) the radiated power ratio as function of the operational frequency for several angular apertures of the funnel ( $a = 2$  mm,  $U = 24$ ), (c) the radiated power ratio as function of the number of pins for various frequencies ( $a = 5$  mm,  $\theta = 60^\circ$ ). Plot parameters:  $\omega_P = 20 \pi$  Grad/sec,  $W = 30$  mm,  $I = 1$  A.

one, regardless of the chosen angle  $\theta$ .

In Fig. 4(c), the quantity  $R$  is represented as function of the number of pins for several oscillation frequencies with fixed angle  $\theta = 60^\circ$ . One can easily observe a relative stability of curves with respect to the population size of the pins. This fact indicates that the drawn conclusions could hold even for moderate number of cylinders. The (anyway slow) variation is even less significant for frequencies closer to plasma limit. As far as the magnitude of  $R$  is concerned, a

substantial performance is recorded for the low frequency  $\omega = 0.75\omega_P$ .

In Fig. 5, we assume the distribution shown in Fig. 5(a) of  $(U - 1)$  vertically posed cylinders together with a regulating pin centered at

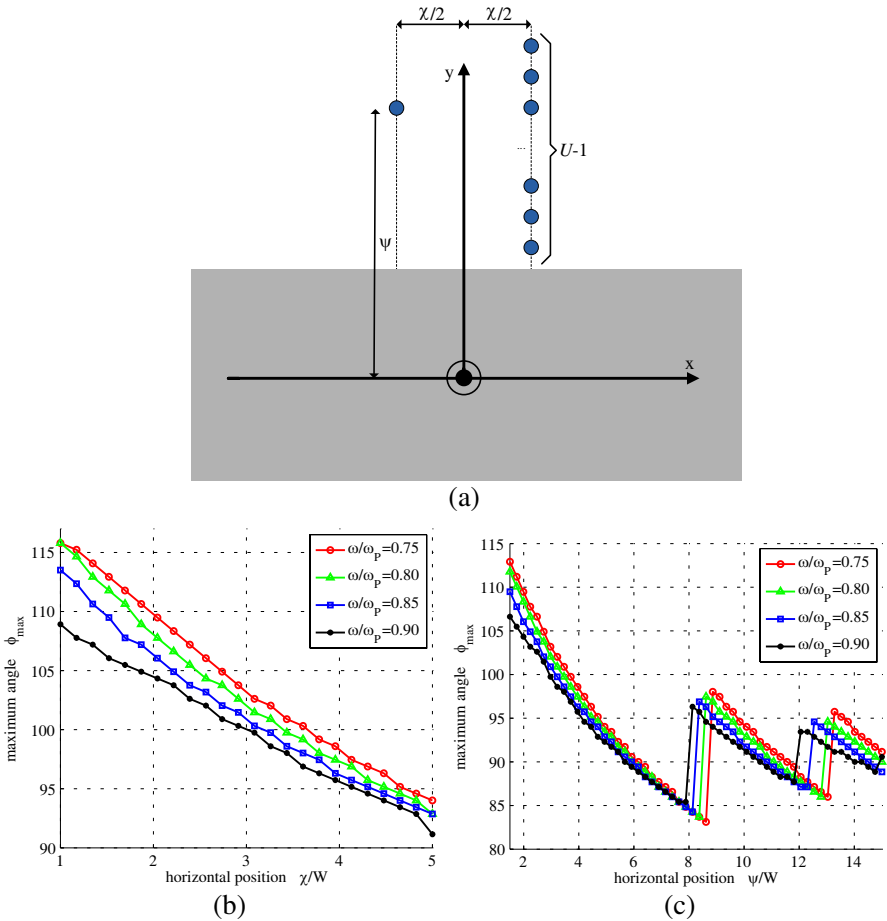


**Figure 5.** (a) The examined case of a vertical distribution of cylinders with one regulating pin, (b) the maximum power angle as function of the horizontal distance between the pin and the cluster for various frequencies ( $\psi = 5W$ ), (c) the maximum power angle as function of the vertical position of the pin for various frequencies ( $\psi = \chi$ ). Plot parameters:  $\omega_P = 20 \pi \text{Grad/sec}$ ,  $a = 5 \text{ mm}$ ,  $W = 30 \text{ mm}$ ,  $I = 1 \text{ A}$ ,  $\theta = 60^\circ$ ,  $U = 15$ .

$(x, y) = (-\frac{\chi}{2}, \psi)$ . The positions of the cylinders are given by:

$$x_u = \frac{\chi}{2}, \quad y_u = W + 3au, \quad (17)$$

for  $u = 1, \dots, (U - 1)$ . In Fig. 5(b), the direction of maximum power is depicted as function of the horizontal position  $\chi$  for various frequencies, with fixed  $\psi$ . When the horizontal distance between the regulating cylinder and the vertical cluster gets increased, the maximum radiation angle is decreasing, tending to  $90^\circ$ . This is an anticipated result, as the farther from the vertical axis the scatterers are located, the less powerful is the field with which the metallic volumes are interacting. The behavior of the four curves are very similar but the deviation of  $\phi_{\max}$  from  $90^\circ$  gets less significant for increasing operational frequencies.

In Fig. 5(c), the same quantity  $\phi_{\max}$  is represented as function of the vertical position  $\psi$ , which is taken equal to (also variable)  $\chi$ . Again, the maximal power direction tends to  $90^\circ$  for  $\chi = \psi \gg W$  because the effect of the scattering lattice gets diminishing. In addition, there is a periodic behavior of the curves with respect to  $\psi$ , which is explained by the oscillatory nature of the EM fields. Mind also the discontinuous behavior of the curves attributed to the features of the function  $\arg\max(z)$ .

#### 4. CONCLUSION

The effect of finite set of metallic pins on the operation of a low-index metamaterial slab antenna has been analyzed in the present work. The boundary value problem is solved approximately, under the reasonable assumption that the electric radius of the perfectly conducting cylinder is small. The obtained results have been validated independently, while the produced diagrams are commented and discussed.

The present study of the effect of the metallic pins on the function of the device, certainly pertains to this specific antenna configuration. However, the drawn conclusions can be generalized to cover larger classes of radiators. In particular, the properties of this additional equipment affecting the considered metamaterial slab antenna, could carry over to other more complicated background radiating structures. The same technique could be also used in examining alternative positioning of the metallic pins and could be expanded to cover configurations with clusters of dielectric cylinders constructed from different materials. Another intriguing elaboration would be the optimization of the desired quantities (radiated power, directivity, etc.) with respect to the positions of the pins, leading to novel applicable structures for antenna devices.

## ACKNOWLEDGMENT

The author is grateful to Dr. Pekka Alitalo for useful advice and discussion.

## REFERENCES

1. Ding, K., T. Jiang, J. Hao, L. Ran, and L. Zhou, "Directional emissions achieved with anomalous reflection phases of metamaterials," *Journal of Applied Physics*, Vol. 107, 2010.
2. Cheng, X., H. Chen, B.-I. Wu, and J. A. Kong, "Cloak for bianisotropic and moving media," *Progress In Electromagnetics Research*, Vol. 89, 199–212, 2009.
3. Duan, Z.-Y., B.-I. Wu, J. A. Kong, F. Kong, and S. Xi, "Enhancement of radiation properties of a compact planar antenna using transformation media as substrates," *Progress In Electromagnetics Research*, Vol. 83, 375–384, 2008.
4. Alitalo, P., O. Luukkonen, and S. A. Tretyakov, "A three-dimensional backward wave network matched with free space," *Physics Letters A*, Vol. 372, 2720–2723, 2008.
5. Shooshitari, A. and A. R. Sebak, "Electromagnetic scattering by parallel metamaterial cylinders," *Progress In Electromagnetics Research*, Vol. 57, 165–177, 2006.
6. Sahin, A. and E. L. Miller, "Recursive T-matrix algorithm for multiple metallic cylinders," *Microwave and Optical Technology Letters*, Vol. 15, 360–363, 1997.
7. Lucido, M., G. Panariello, and F. Schettino, "Electromagnetic scattering by multiple perfectly conducting arbitrary polygonal cylinder," *IEEE Transactions on Antennas and Propagation*, Vol. 56, 425–436, 2008.
8. Habib, M. A., A. Bostani, A. Djaiz, M. Nedil, M. C. E. Yagoub, and T. A. Denidni, "Ultra wideband CPW-FED aperture antenna with WLAN band rejection," *Progress In Electromagnetics Research*, Vol. 106, 17–31, 2010.
9. Mahmoud, K. R., "Design optimization of a bow-tie antenna for 2.45 GHz RFID readers using a hybrid BSO-NM algorithm," *Progress In Electromagnetics Research*, Vol. 100, 105–117, 2010.
10. Jin, X. and M. Ali, "Embedded antennas in dry and saturated concrete for application in wireless sensors," *Progress In Electromagnetics Research*, Vol. 102, 197–211, 2010.
11. Bucci, O. M., T. Isernia, and A. F. Morabito, "A deterministic approach to the synthesis of pencil beams through planar thinned

- arrays,” *Progress In Electromagnetics Research*, Vol. 101, 217–230, 2010.
12. Tze-Meng, O., K. G. Tan, and A. W. Reza, “A dual-band omnidirectional microstrip antenna,” *Progress In Electromagnetics Research*, Vol. 106, 363–376, 2010.
  13. Chang, T. N., G. Y. Shen, and J. M. Lin, “CPW-fed antenna covering wimax 2.5/3.5/5.7 GHz bands,” *Journal of Electromagnetic Waves and Applications*, Vol. 24, No. 2–3, 189–197, 2010.
  14. Ouyang, j., F. Yang, H. Zhou, Z. Nie, and Z. Zhao, “Conformal antenna optimization with space mapping,” *Journal of Electromagnetic Waves and Applications*, Vol. 24, No. 2–3, 251–260, 2010.
  15. Chen, J., G. Fu, G.-D. Wu, and S.-X. Gong, “Compact graded central feeder line CPW-fed broadband antenna,” *Journal of Electromagnetic Waves and Applications*, Vol. 23, 2089–2097, 2009.
  16. Hwang, R.-B., H.-W. Liu, and C.-Y. Chin, “A metamaterial-based  $E$ -plane horn antenna,” *Progress In Electromagnetics Research*, Vol. 93, 275–289, 2009.
  17. Sabah, C. and S. Uckun, “Multilayer system of Lorentz/Drude type metamaterials with dielectric slabs and its application to electromagnetic filters,” *Progress In Electromagnetics Research*, Vol. 91, 349–364, 2009.
  18. NaghshvarianJahromi, M., “Novel compact metamaterial tunable quasi elliptic band-pass filter using microstrip to slotline transition,” *Journal of Electromagnetic Waves and Applications*, Vol. 24, 2371–2382, 2010.
  19. Mirzavand, R., B. Honarbakhsh, A. Abdipour, and A. Tavakoli, “Metamaterial-based phase shifters for ultra wide-band applications,” *Journal of Electromagnetic Waves and Applications*, Vol. 23, No. 11–12, 1489–1496, 2009.
  20. Oraizi, H. and A. Abdolali, “Some aspects of radio wave propagation in double zero metamaterials having the real parts of epsilon and mu equal to zero,” *Journal of Electromagnetic Waves and Applications*, Vol. 23, No. 14–15, 1957–1968, 2009.
  21. Jarchi, S., J. Rashed-Mohassel, and R. Faraji-Dana, “Analysis of microstrip dipole antennas on a layered metamaterial substrate,” *Journal of Electromagnetic Waves and Applications*, Vol. 24, No. 5-6, 755–764, 2010.
  22. Costanzo, S., “Synthesis of multi-step coplanar waveguide-to-

- microstrip transition,” *Progress In Electromagnetics Research*, Vol. 113, 111–126, 2011.
23. Marynowski, W., P. Kowalczyk, and J. Mazur, “On the characteristic impedance definition in microstrip and coplanar lines,” *Progress In Electromagnetics Research*, Vol. 110, 219–235, 2010.
  24. Sim, C.-Y.-D., W.-T. Chung, and C.-H. Lee, “Planar UWB antenna with 5 GHz band rejection switching function at ground plane,” *Progress In Electromagnetics Research*, Vol. 106, 321–333, 2009.
  25. Carretero, C., R. Alonso, J. Acero, and J. M. Burdío, “Coupling impedance between planar coils inside a layered media,” *Progress In Electromagnetics Research*, Vol. 112, 381–396, 2011.
  26. Sze, J.-Y. and Y.-F. Wu, “A compact planar hexa-band internal antenna for mobile phone,” *Progress In Electromagnetics Research*, Vol. 107, 413–425, 2010.
  27. Liu, Y., X. Chen, and K. Huang, “A novel planar printed array antenna with SRR slots,” *Journal of Electromagnetic Waves and Applications*, Vol. 24, No. 16, 2155–2164, 2010.
  28. Zhan, K., Q. Guo, and K. Huang, “A miniature planar antenna for bluetooth and UWB applications,” *Journal of Electromagnetic Waves and Applications*, Vol. 24, No. 16, 2299–2308, 2010.
  29. Valagiannopoulos, C. A., “A novel methodology for estimating the permittivity of a specimen rod at low radio frequencies,” *Journal of Electromagnetic Waves and Applications*, Vol. 24, No. 5–6, 631–640, 2010.
  30. Valagiannopoulos, C. A., “On developing alternating voltage around a rotating circular ring under plane wave excitation in the presence of an eccentrically positioned metallic core,” *Progress In Electromagnetics Research M*, Vol. 12, 193–204, 2010.
  31. Pacheco, J., “Theory and application of lefthanded metamaterials,” 181–216, Ph.D. Dissertation, MIT, Cambridge, MA, 2004.
  32. Axelrod, N. N. and P. M. Givens, “Optical measurement of the plasma frequency and  $M_{2,3}$  band of chromium,” *Physical Review*, Vol. 120, No. 4, 1205–1207, 1960.
  33. Wills, R. C., M. Davis, P. P. Woskov, J. Kesner, D. T. Garnier, and M. E. Mauel, “Density profile measurements in LDX using microwave reflectometry,” *MIT Plasma Science and Fusion Center Library*, No. RR-10-9, 2010.
  34. Valagiannopoulos, C. A., “Electromagnetic scattering from two eccentric metamaterial cylinders with frequency-dependent per-

- mittivities differing slightly each other,” *Progress In Electromagnetics Research B*, Vol. 3, 23–34, 2008.
35. Valagiannopoulos, C. A., “Effect of cylindrical scatterer with arbitrary curvature on the features of a metamaterial slab antenna,” *Progress In Electromagnetics Research*, Vol. 71, 59–83, 2007.
  36. Valagiannopoulos, C. A., “On developing alternating voltage around a rotating circular ring under plane wave excitation in the presence of an eccentrically positioned metallic core,” *Progress In Electromagnetics Research M*, Vol. 12, 193–204, 2010.
  37. Valagiannopoulos, C. A., “On examining the influence of a thin dielectric strip posed across the diameter of a penetrable radiating cylinder,” *Progress In Electromagnetics Research C*, Vol. 3, 203–214, 2008.
  38. Erdelyi, A., *Asymptotic Expansions*, Dover Publications, New York, 1956.